Article

Rapid ecological change outpaces climate warming in Tibetan glacier lakes

Check for updates

Chenliang Du [1,5], Ke Zhang [2,5] ✉, Qi Lin [2], Shixin Huang [1], Yaoyao Han[2], Junming Ren[1], Peng Xing [2], Jianbao Liu [3], David Taylor[4] & Ji Shen [1] ✉

The rapid warming of the Tibetan Plateau, at more than twice the global average, raises urgent questions about how quickly alpine aquatic ecosystem can respond. Here, using lake sedimentary ancient DNA (*sed*aDNA) and photosynthetic pigment analysis, we investigated algal productivity and diversity (alpha, beta) changes in a Tibetan glacier lake, Guozha Co, China, and by integrating regional lake records, we further estimated the rate of change (RoC) associated with lake ecosystem and temperature over the past two centuries. Our findings reveal that while the RoC of algal communities historically tracked temperature trends, a significant divergence emerged in the 1980s, with the ecological RoC surpassing that of climate warming. The observed shift from cold-tolerant to warm-adapted algal species, alongside enhanced primary productivity, is closely linked to rising temperatures and the cascading effects of glacier retreat. This rate mismatch signals a significant disruption in the long-standing equilibrium between climate and aquatic ecosystems, with potentially far-reaching consequences for alpine biodiversity conservation under accelerating global change.

Accelerating anthropogenic global warming is driving the swift expansion of glacial lakes globally, leading to profound societal and ecological impacts[1,2]. The Tibetan Plateau (TP), known as the "Water Tower of Asia", is notable for its extensive alpine lake systems, comprising over 5700 glacier lakes at an average elevation of 4500 meters above sea level, which serve as a crucial water source for nearly 2 billion people across Asia[3,4]. Notably, the TP has experienced warming at a rate more than twice the global average in recent decades[5,6]. This pronounced warming has triggered profound transformations in glacier lakes, particularly in the northwestern TP[7]. These changes encompass marked increases in lake volume[8,9], accelerated rises in surface water temperature[10,11], shifts in lake ice phenology[12] and more frequent, abrupt glacier lake outburst[13,14]. Furthermore, this warming has prompted hydrological reorganization[15] and the emergence of new ecosystems[16,17] on the TP. Despite the recognized vulnerability of these glacial lake ecosystems to climate change and their critical roles in biomass production, biodiversity, and carbon sequestration[18], the degree to which they have responded to the rapid warming remains largely unexplored.

Ecosystems response to climate change are varied[19]. Some ecosystems manage to keep pace with climate shifts and maintain a dynamic equilibrium with their surroundings[20,21]; while others may either lag climate forcing[22–25], or exhibit abrupt, nonlinear, threshold-type responses[26]. This mismatch between the rate of change (RoC) in the climate driver and

ecosystem response can result in ecological debts[27], species extinction, invasion[28], range shifts[29], network instability[30], and potentially irreversible ecological transformations[31]. Warming is widely reported to have increased species richness while decreasing beta diversity[32], and have driven transitions from cold-adapted to warm-adapted taxa in eukaryotic communities and from benthic to planktonic species in lentic ecosystems[33,34]. With the prospect of accelerating future warming, the disparity between the RoC of ecosystems and that of climate is expected to grow, presenting unpredictable consequences[35].

There is an emerging consensus on the need to understand the dynamic RoC relationships between ecosystems and their environmental stressors to navigate the challenges of accelerated warming effectively[26,36]. However, most existing studies tend to exclusively focus on the RoC of climate[6,37], or the RoC of ecosystems separately[20,36], with limited information available about long-term dynamic, interacting relationships between the two, particularly referring to fragile, high alpine aquatic ecosystems[38]. The scarcity of in-situ observations and the lack of multi-decadal records have further limited our ability to examine these dynamics during the recent period of anthropogenic warming[39]. Recent methodological advances in paleolimnology, particularly *sed*aDNA and photosynthetic pigment have greatly improved our ability to provide detailed insight at high taxonomic resolution into past diversity changes[40–42].

[1]School of Geography and Ocean Sciences, Nanjing University, Nanjing, China. [2]State Key Laboratory of Lake and Watershed Science for Water Security, Nanjing Institute of Geography and Limnology, Chinese Academy of Sciences, Nanjing, China. [3]State Key Laboratory of Tibetan Plateau Earth System Science, Institute of Tibetan Plateau Research, Chinese Academy of Sciences, Beijing, China. [4]Department of Geography, National University of Singapore, Singapore, Singapore. [5]These authors contributed equally: Chenliang Du, Ke Zhang. ✉e-mail: kzhang@niglas.ac.cn; jishen@nju.edu.cn

In response to this gap, we employed a retrospective approach using sediment archives, to reconstruct the long-term trajectories of algal production, community composition, and their alpha and beta diversity based on *sed*aDNA and pigments from Guozha Co, a typical glacier-fed lake on the northwest Tibetan Plateau, located approximately 20 kilometers south of the West Kunlun Mountain Glacier (Fig. 1). By conducting a comparative analysis of the RoC in the algal community with that of climate records, together with the integration of remote sensing data and paleoecological

records at larger spatial scale, we aim to investigate whether recent anthropogenic warming after 1850 CE is paralleled by similar accelerations in glacier-fed lake ecosystems. Specifically, we seek to determine the pace at which these aquatic ecosystems have adapted to climatic warming over the past two centuries and to identify the underlying mechanisms driving these changes. This study highlights the importance of examining the relationship between the RoC in climate and alpine lake ecosystems to better understand their vulnerability and resilience to ongoing climatic shifts.
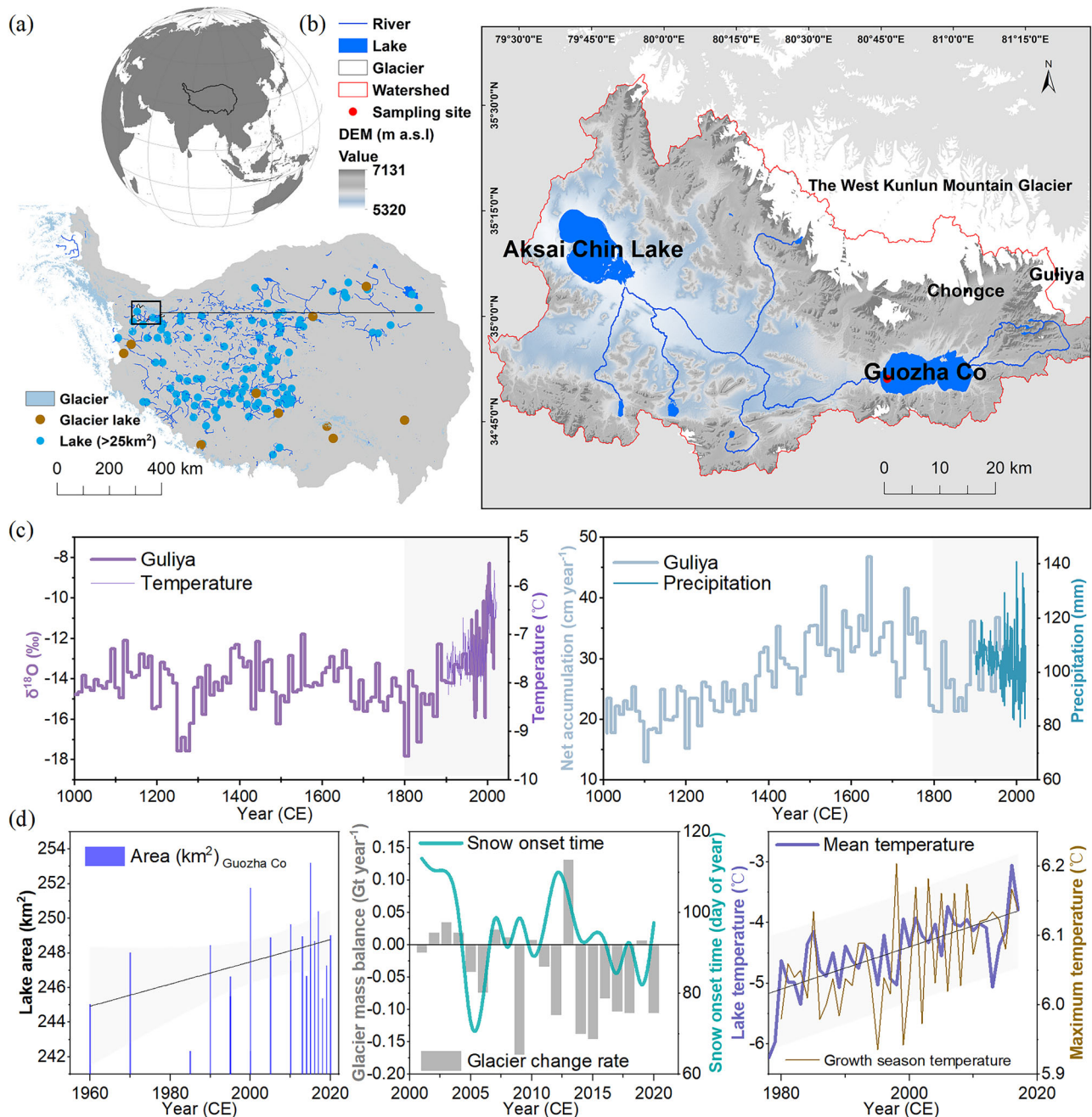

Fig. 1 | Overview of study sites and regional environmental datasets. a Geographic distribution of lakes analyzed in this study, differentiated by glacier-fed lakes (brown markers) and large lakes (area > 25 km², blue markers) as identified in prior research (for data sources, refer to Supplementary Table 4, 5). **b** Detailed map showing the location of Guozha Co, including the sediment core collection site, with black dots marking the ice caps (Guliya and Chongce) of the West Kunlun Mountain Glacier. Maps were created in ArcMap 10.3.1 software. **c** Composite chart displaying regional

temperature (δ¹⁸O) and precipitation (glacier net accumulation) trends derived from Guliya ice core analyses spanning the last millennium[96–99], complemented by recent temperature and precipitation measurements from the catchment (http://www.cru.uea.ac.uk/). **d** Visual summary of recent climatic impacts on the glacier-lake system, showcasing data on glacier change rate, changes in snow onset timing, lake area expansion, and lake surface temperature fluctuations (detailed sources in Supplementary Table 4).

Results

Chronology and geochemical results

Chronological sequences were constructed based on the radioactivities of bulk sediment ^{210}Pb and ^{137}Cs measurements. The exponential decrease in excess ^{210}Pb (^{210}Pb$_{ex}$) activities reached secular equilibrium at approximately 11 cm depth (Supplementary Fig. 1). A distinct ^{137}Cs peak at 7 cm depth corresponded to the 1963 CE atmospheric fallout from nuclear weapons tests[43,44]. The ^{137}Cs-corrected Constant Rate of Supply (CRS) model was applied to develop the age model, and revealed the upper 11 cm of the sediment core represents the past ~150 years, approximately spanning from ~1860 CE (95% confidence interval (CI), ±14 years) to the collection date in 2021. Ages below 11 cm, down to the core's base at 39 cm, were linear extrapolated and calibrated based on previous results[45], dating the bottom to around ~1000 CE (mean error of ~65 years over the past millennium)[45]. A more detailed examination of the sediment chronology is provided in the Supplementary Note 1. This study primarily focused on the past ~200 years to explore the RoC relationships between recent anthropogenic warming and aquatic ecological transformations.

The geochemical analysis of the GZC-21 core revealed a sediment composition predominantly characterized by silt (2 μm < grain size < 63 μm, 66.89%) and sand (grain size > 63 μm, 24.87%)[45] (Supplementary Note 2). The results of coarse particle components (> 63 μm, rising from 15.63% to 30.26%), major and trace elements PC1 scores (rising from −0.52 to 1.62) and magnetic susceptibility (rising from 7.40 to 8.80 × 10^{-8} m^3 kg^{-1}) over the past ~100 years indicated marked increases in watershed runoff and hydrodynamic activity, pointing to heightened terrigenous clastic input (Supplementary Fig. 2, 3). Additionally, the high Fe/Mn ratio and reduced salinity (as indicated by Sodium (Na) concentrations) during the recent century suggested elevated lake levels and increased freshwater input, likely driven by enhanced glacier meltwater inflow. Current Chl-a concentration of the lake water body is approximately 3 μg L^{-1}, reflecting relatively low lake productivity and limited organic matter inputs from the barren watershed[46]. Correspondingly, the sediment exhibited relatively low levels of total organic carbon (TOC) and total nitrogen (TN), with mean values of 0.34% and 0.05%, respectively. Notably, TOC and TN levels increased from the early 1900 CE, rising from 0.30% to 0.43% and 0.05% to 0.07%, respectively. The C/N ratios were rather low and fluctuated around mean value of 7.52, with notable peaks at ~1500 CE and after ~1900 CE (Supplementary Fig. 2). These values probably suggested a predominance of autochthonous (endogenous) organic matter sources and slight increases in terrigenous inputs and autochthonous production, as supported by C/N ratios consistently below 8. Total phosphorous concentrations (mean values ranging from 566.78 mg kg^{-1} to 532.84 mg kg^{-1}) exhibited a decline starting in the mid-core period (~1600 CE), followed by a gradual increase in recent centuries. This pattern likely reflected changing nutrient inputs over time. Results of regime shift based on major sediment physicochemical records further highlighted that lake-watershed system experienced abrupt environmental changes within the last century, underscoring the profound impacts of recent aquatic ecological transformations (Supplementary Fig. 2; black lines).

Algae community diversity, composition, and rate of change

Algal pigment analysis mirrored geochemical trends, revealing an increase in biomass over the last century (Fig. 2a). The concentrations of key photosynthetic pigments, including those indicative of total algae abundance (Chl-a, pheophytin-a and its deviation pheophytin-a'), siliceous algae (diatoxanthin), chlorophytes (lutein, pheophytin-b and its deviation pheophytin-b'), and cyanobacteria (canthaxanthin), remained stable but low prior to ~1900 CE, with a notable increase thereafter (Fig. 2a). Furthermore, a stable increasing ratio of chlorophyll-a to pheophytin-a (Chl-a/Pheo-a) in the upper core reflected slightly improved pigment preservation when algal production increases, especially after 1950 CE (see Supplementary Note 3 and Supplementary Fig. 4 for detailed interpretation of the sedimentary pigment preservation). The chlorophytes had the highest concentrations (25.51–149.37 nmole pigment g^{-1} TOC), followed by

siliceous algae (2.78–48.85 nmole pigment g^{-1} TOC) and cyanobacteria (0.28–3.07 nmole pigment g^{-1} TOC). Generalized additive models (GAM) applied to temporal variations in algal abundances highlighted a significant biomass increase for siliceous algae ($p < 0.001$, $R_{Adj}^2 = 0.93$), chlorophytes ($p < 0.001$, $R_{Adj}^2 = 0.81$), and total algae ($p < 0.001$, $R_{Adj}^2 = 0.75$) over the past millennium, with siliceous algae exhibiting particularly rapid growth (mean increase from 6.36 to 32.80 nmole pigment g^{-1} TOC) (Supplementary Fig. 5).

The sedaDNA results provided higher taxonomic resolution compared to pigment analyses, enabling enhanced detection of indicative species and a more refined interpretation of community dynamics. A total of 1603,115 and 1571,225 high-quality sequences of 18S rRNA and 16S rRNA were obtained from 27 sedimentary samples, corresponding to 393 and 2220 OTUs for eukaryotes and bacterium, respectively. Sequencing yielded 301,324 reads for eukaryotic algal communities and 4,750 reads for cyanobacterial communities, identifying 64 and 36 OTUs, respectively, for bioinformatic analyses. Taxonomic data cleaning and filtering were conducted using the SILVA reference sequence database, applying a confidence threshold of ≥ 80% (Supplementary Table 1). Combined with sedimentary pigment results (Fig. 2a), sedaDNA rarefaction curves (Supplementary Fig. 6), and OTU counts (Supplementary Fig. 7) indicated sufficient diversity estimates for reliable analysis, while also observing limited DNA degradation at the millennial scales (Supplementary Note 4, Supplementary Fig. 7). All blanks were found negative in this study (Supplementary Fig. 8, 9). At the phylum level, the relative abundances (%) of algal taxa determined by reads were basically consistent with sedimentary pigments, with mean value of 72.99% for chlorophytes, 14.92% for siliceous algae, 8.55% for ochrophyta, and 3.53% for cryptophyceae (Supplementary Fig. 10). Cyanobacteria consistently appeared at low abundance (4370 reads) across the sedimentary profiles (Supplementary Table 1).

We focused on the genera assigned to eukaryotic algae and cyanobacteria, which included *Chlorophyceae* (53.21%), *Trebouxiophyceae* (18.77%), *Fragilariales* (10.47%), *Cyanobium* (63.39%), and *Chloroplast* (17.53%), which were relatively abundant in the lake (Fig. 2b). Notably, the alpha diversity (Shannon index) marked an increase in the richness of eukaryotic algal communities in recent two centuries (Supplementary Fig. 11). Temporal variations in beta diversity (NMDS1) showed similar fluctuations to alpha diversity, peaking around 2000 CE (Supplementary Fig. 12). Although the presence of 0 values in the OTU data might have caused the first axis to explain only 42.15% of the total variance, the sedaDNA data still revealed identified significant beta-diversity changes in eukaryotic communities after 1900 CE, as captured by PCoA analysis (ANOVA test of first axis, $p < 0.001$; Supplementary Fig. 13, 14) and PERMANOVA test (Supplementary Table 2, $p < 0.001$). Additionally, NMDS analysis also showed significant differences (Supplementary Figs. 15–17, $p < 0.001$). These changes were associated with an increased abundance of *Fragilariales* (*Skeletoneme* sp., tolerate low salinity) and a decrease in cold-tolerant genera, such as *Chlorophyceae*, *Trebouxiophyceae*. As shown in the SEM (Structural equation modeling) results, the glacier lake ecosystem was mainly influenced by glacial meltwater ($r = 0.746$, $p < 0.001$), precipitation ($r = 0.171$, $p < 0.05$), and solar radiation ($r = 0.153$, $p < 0.05$) in cold periods, with temperature having an insignificant effect ($r = 0.002$, $p > 0.05$). Under accelerated warming in recent decades, however, ecosystem changes are increasingly driven by glacial meltwater ($r = 0.701$, $p < 0.001$) and temperature ($r = 0.247$, $p < 0.05$), with temperature-induced glacier melting becoming a significant factor ($r = 0.363$, $p < 0.05$) in warm periods. The PERMANOVA test revealed significant differences in cyanobacteria communities before and after 1900 CE (Supplementary Table 3, $p = 0.007$). Meanwhile, we observed an increase in the fluctuations of *Candidatus* sp. abundance, with its mean value of relative abundance rising from 3.50% to 15.47% over the past two centuries.

Results of sedaDNA and pigments analyses showed similar fluctuations, enhancing the reliability of multi-proxy comparison for ecological-climatic contrast (Fig. 3a). RoC revealed a significant acceleration in ecological change in the lake over the past millennium, particularly since the
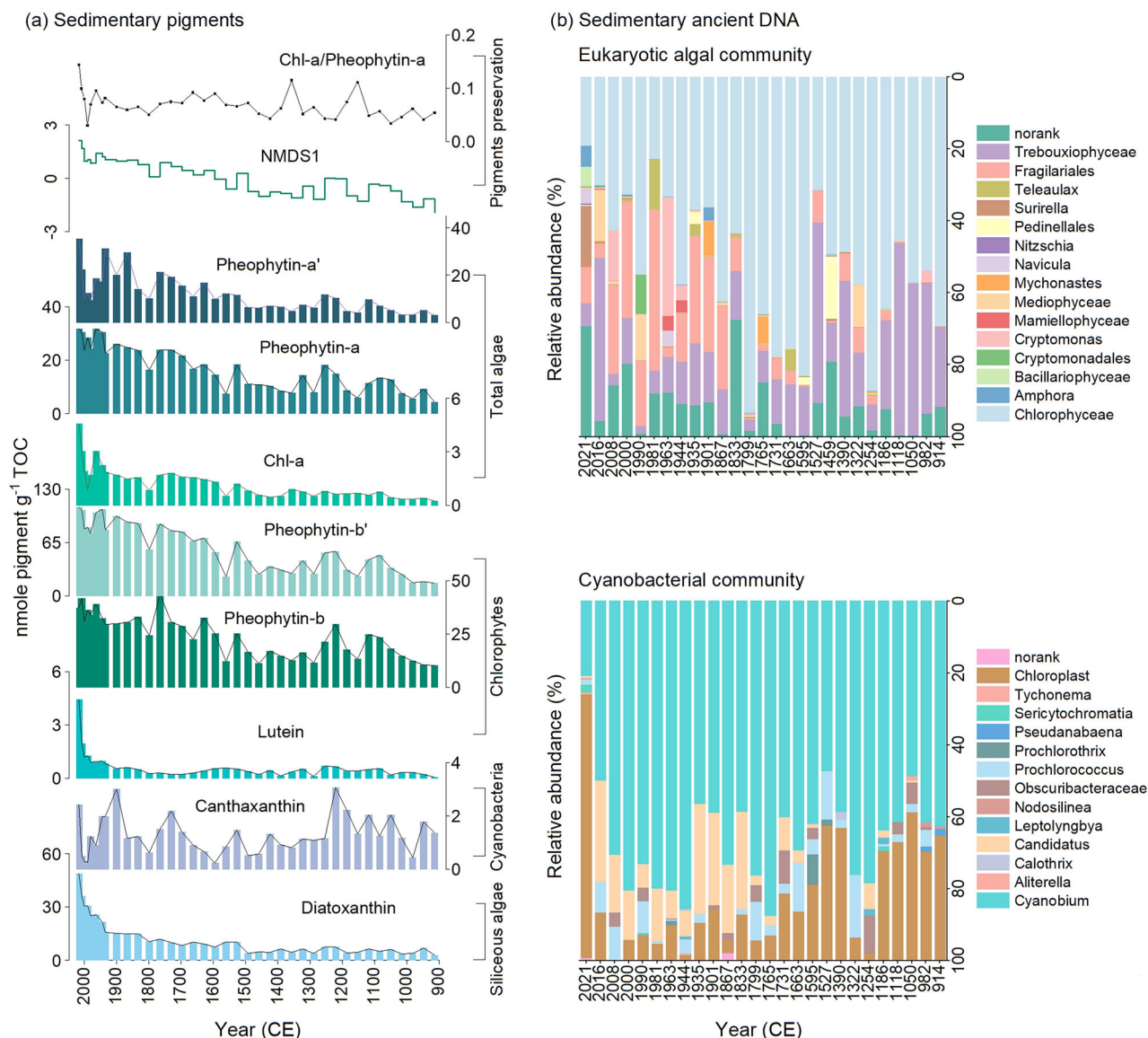
Fig. 2 | Sedimentary pigments and ancient DNA records from Guozha Co.
a Temporal changes in concentrations of main sedimentary pigments (nmole pigment g^{-1} TOC). Subfossil pigment types include diatoxanthin from siliceous algae, canthaxanthin from cyanobacteria, lutein, pheophytin-b and its derivative pheophytin-b' from chlorophytes, and total algae (Chl-a, pheophytin-a and its derivative pheophytin-a'). The preservation conditions of pigments are represented by Chl-a/Pheo-a and the overall algal community as indicated by the NMDS1 scores (Supplementary Fig. 12, 15). **b** Sedimentary ancient DNA (*sed*aDNA) shift depicted via the relative abundance (%) of eukaryotic algae and cyanobacterial communities at the genus level.

mid-20th century (Supplementary Fig. 18, Supplementary Note 5). This acceleration was evident across key ecological indicators after ~1960 CE, such as primary production of siliceous algae (diatoxanthin), total algae (Chl-a, pheophytin-a and its deviation pheophytin-a'), and TOC (Fig. 3a; red lines). Species richness, including alpha diversity (Shannon index) and beta diversity (NMDS1), also showed an increasing trend. This upsurge correlates with significant RoC increases in temperature over the same period. The mean RoC for both ecosystem and climate data, assessed per five-decade intervals, remained relatively stable before 2000 CE but demonstrated a sharp rise in the recent two decades (t-test; $p < 0.001$) (Supplementary Fig. 19). There was a significant difference (ANOVA; $p < 0.001$) in the rates of climate and ecosystem change during in period after 2000 CE (Fig. 3b). A critical observation from the RoC analysis was the close tracking (around the 1:1 line) of ecosystem changes with regional warming over the last century. However, a divergence occurred around 1980–1990 CE, where the RoC for the ecosystem surpassed that of the climatic variables, indicating a faster rate of ecological change compared to

regional warming. The bi-plot of RoC for the ecosystem against that of the climate deviated significantly from the equilibrium line around 1980 CE (Fig. 3c). The rate of ecological change fitted by the GAM exhibited this significantly divergence from that of warming ($R_{Adj}^2 = 0.574$, $p < 0.001$), further supporting the conclusion of ecosystem shift more rapidly than climate change (Fig. 3c; black solid line). The regional integration results (meta-analysis), including HGAM fitting of paleoecological proxies from multiple lakes (Fig. 4a; $R_{Adj}^2 = 0.30$, $p < 0.001$) and the FUI index (Fig. 4b; $R_{Adj}^2 = 0.17$, $p < 0.001$), supported a consistent increase in ecological RoC after ~1960 CE across the Tibetan glacier lakes (Fig. 4c; red lines), with further fluctuation and rise in recent decades (Fig. 4d, Supplementary Note 6).

Discussion
Our research illuminates the profound pace at which alpine glacier-fed lake ecosystems are responding to accelerating anthropogenic warming, with implications critical for biodiversity and ecosystem conservation. By
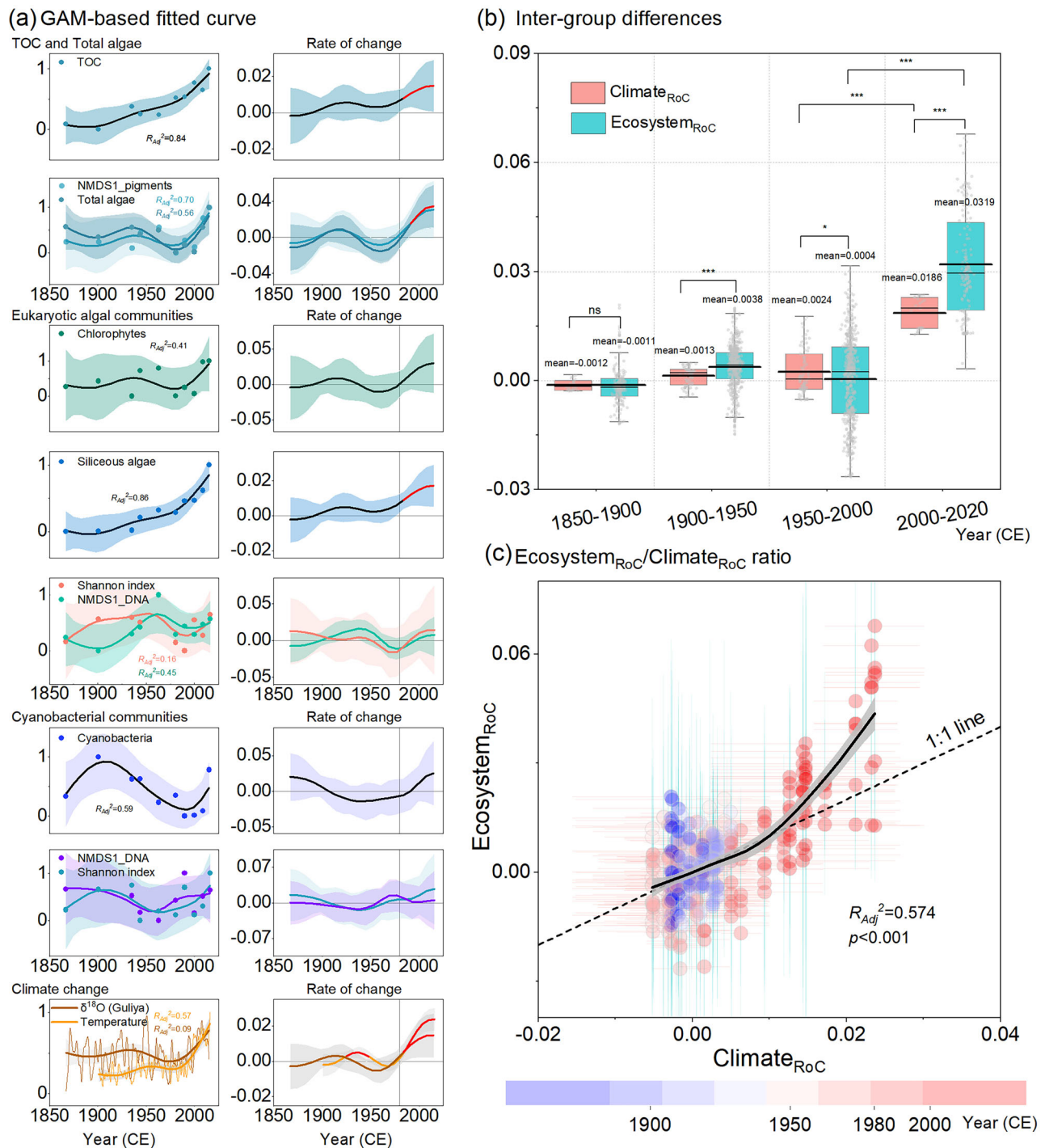
Fig. 3 | Analysis of rate of change (RoC) in algal production and diversity relative to climate change. a GAM-based time series representations of ecosystem (TOC, pigments and algal diversity from *sed*aDNA) and climate dynamics (regional temperature from instrument measurement, modeling and ice $\delta^{18}O$ reconstruction), respectively, alongside their corresponding RoC, with 95% simultaneous confidence intervals (CI) depicted by color ribbons, with red lines marking significant acceleration (the 95% CI do not encompass zero) of phytoplankton abundance and temperature warming within the past two centuries. The horizontal dashed line is located to distinguish between acceleration and deceleration (RoC = 0). Ecosystem and climatic RoC for statistical analysis in (**b**) and (**c**) were generated based on multivariate rate calculations in (**a**). **b** Comparative statistics highlighting all RoC values summarized within climate and ecosystem across distinct timeframes. Black

lines mark the mean values, while illustrate the disparity in RoC between climate and ecosystem, emphasizing periods of significant divergence. Parentheses with significance markers indicate differences between any two groups, based on ANOVA analysis. The significance levels are *$p < 0.05$, **$p < 0.01$, ***$p < 0.001$. **c** The ratio of RoC between ecosystem and climate on a 1:1 scale, illustrating the relative pace of change in each domain. Gradient color scatters denote the dynamic of RoC over time at different periods. The black dashed line represents the 1:1 line, while the black solid line shows the GAM-fitted result for the scatter points. The RoC of climate change as the independent variable (predictors) and the rate of ecological change as the dependent variable (responses). The gray shading indicates the 95% CI. The red horizontal error bars represent the uncertainty of the climate rate (95% CI), and the light blue vertical error bars represent the uncertainty of the ecological rate (95% CI).
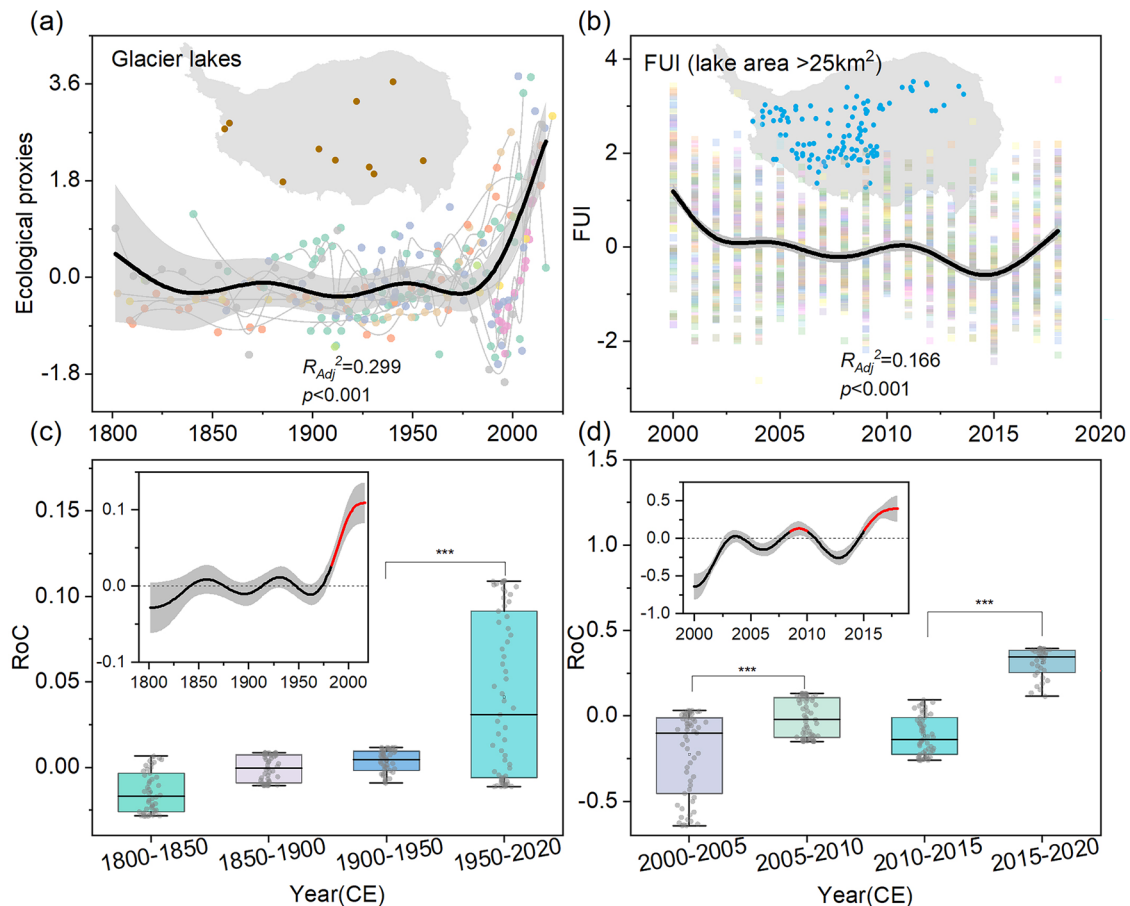
Fig. 4 | Regional integrated analysis of paleoecological records and remote sensing data across the Tibetan Plateau lakes. a, c show sedimentary proxies aggregated from approximately 10 glacier-fed lakes on the Tibetan Plateau (TP), illustrating the rate of change (RoC) derived from curves fitted with hierarchical generalized additive models (HGAM). For detailed data, refer to Supplementary Table 5. This panel visualizes the synthesized RoC across selected lakes, underlining the widespread ecological shifts within the region. **b, d** show analysis of the Forel-Ule Index (FUI), a holistic indicator of lake water quality, across 111 large lakes (lake area > 25 km²) on the TP, modeled using HGAM to determine its RoC. Similarly, temporal RoC in regional lake paleoecological records and FUI time series was estimated from the posterior simulations of the fitted HGAMs using the first derivative of a spline, with red lines marking significant acceleration (the 95% CI do not encompass zero). The adjacent box plot emphasizes the variations in RoC during distinct historical periods, showcasing the temporal shifts in lake water quality and environmental conditions across the Tibetan Plateau. Parentheses with significance markers indicate differences between any two groups, based on ANOVA analysis. The significance levels are $*p < 0.05$, $**p < 0.01$, $***p < 0.001$.

conducting a direct comparison of the RoC in both climate and aquatic ecological responses on the TP, with a focus on the past two centuries, we have identified a notable divergence. The RoC of the algal community, initially in sync with climatic trends, has escalated exponentially since the 1960s. This surge has intensified in recent decades, with the ecological RoC eclipsing the pace of climate change from the 1980s onward. This observation is reinforced by a comprehensive regional synthesis of paleoecological records, illustrating profound ecological transformations within lake ecosystems over the last century. Further validation comes from an array of evidence, including published studies[34,47–50], and remote sensing data, collectively highlighting the unparalleled current dynamics between climate and ecology in these glacier-fed lakes. Our findings indicates that the long-standing dynamic equilibrium in glacial lakes, vital for the sustainability of the alpine region's ecological-climate systems for centuries, is now being disrupted, signaling a critical phase of disequilibrium in the evolution of alpine biodiversity.

The long-term consequences of the accelerating changes in algal communities remain uncertain, but the potential for far-reaching effects across the alpine aquatic ecosystems is notable. Phytoplankton, as the primary contributors to primary productivity in alpine lake ecosystems, play a pivotal role in biogeochemical and carbon cycling processes[51]. The varying RoC observed among eukaryotic and cyanobacteria communities may indicate differences in the metabolism and kinetics of biochemical reactions within individual organisms under climate warming[52]. Eukaryotes exhibited a higher temporal turnover rate than bacteria[53]. This could lead to increased competition among algal species and inevitably result in changes in species diversity. Under resource-limited conditions, species with faster growth rates and more efficient resource-utilization strategies gain a competitive edge. As reported and also observed in our study, eukaryotes (especially dinoflagellates and diatoms) that have gradually replaced chlorophytes[34] are the initial competitors and beneficiaries of nitrogen and phosphorus inputs into lakes. Secondary producers (heterotrophic bacteria) are affected subsequently[53]. Cold-preferred species may experience a narrowing of their ecological niches, while warm-preferred species exhibit greater flexibility[33]. For instance, recent transitions from benthic to plankton-dominated assemblages have been documented with the onset of warming in lakes on the southeastern Tibetan Plateau[48]. Others have also observed increases in species diversity, assemblage turnover and replacement[33,54], and faster RoC in glacier lake ecosystems in recent decades[55]. Our findings also indicate a decreased in cold-tolerant species, such as *Trebouxiophyceae*, and concomitant increase in low salinity-tolerant species of *Fragilariales*[56,57], following the transition from cold to warm-humid climate. Furthermore, a rapid RoC of primary producers can disproportionately affect slower-growing zooplankton taxa, potentially disrupting the established aquatic
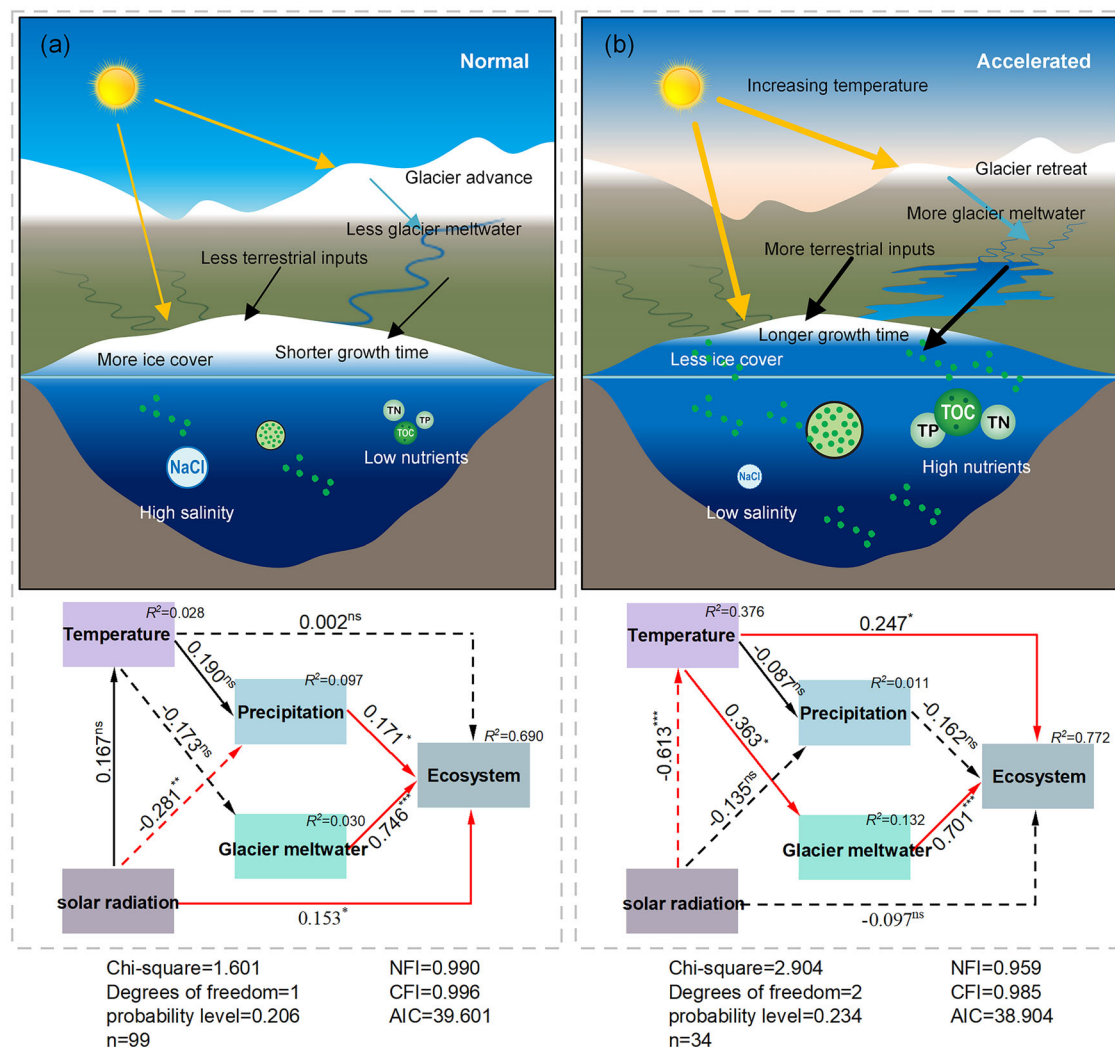
Fig. 5 | Conceptual framework of glacier lake ecosystem dynamics via structural equation modeling. This figure offers a visual schematic and their statistical relations based on SEM analyses, depicting the state of the glacier lake ecosystem under varying rates of ecological response relative to the pace of climate change. Panels **a**, **b** delineate the ecosystem's condition in two distinct phases: the normal phase (prior to ~1980s) and the accelerated phase (post- ~1980s), respectively. **a** In the normal phase, the ecosystem and climate changes are in relative equilibrium, with the thickness of arrow segments representing the moderate strength of ecological driving forces. **b** The accelerated phase shows intensified ecological responses to climate change, highlighted by thicker arrow segments that denote increased force strengths. The color arrows signify the primary drivers within the lake ecosystem (the sum of total algae pigment concentrations), with adjacent numbers quantifying the impact magnitude of each driver. Continuous arrows indicate positive effect while dashed arrows indicate negative effect. The red and black color show significant ($*p < 0.05$, $**p < 0.01$, $***p < 0.001$) and not significant (ns) path, respectively (see Supplementary Fig. 25 and Supplementary Table 7 for more statistical parameters). Goodness of fit statistics are evaluated as follows: Chi-square, Degrees of freedom, probability level, NFI (Normed fit index), CFI (Comparative fit index), AIC (Akaike information criterion), etc. For comprehensive data and a more detailed explanation of these dynamics, refer to the Supplementary Note 10.

food webs[54,58,59]. Given the comparatively limited species pool and simplistic food webs in Tibetan alpine lakes[60], these ecological interactions are of particular concerns, as they could precipitate the loss of endemic species and trigger persistent instability or alternative stable states[61]. Our RoC findings serve not only to document these changes but also to act as harbingers for potential critical transitions within these aquatic ecosystems[62].

The observed acceleration in the algal community dynamics of glacier-fed lakes can be attributed to a confluence of stressors intensified by global warming (Fig. 5). Glacier-fed lake ecosystems are more sensitive to temperature and face heightened vulnerability in the context of rapid global warming, compared to non-glacier fed lakes[63]. The glacier dynamics show that mass loss rates on the TP have persistently increased since the 1960s, and its effects can serve as a critical signal of change in lake ecosystem[64]. For instance, in addition to the direct effects of rising atmospheric temperatures on aquatic organisms, the augmented runoff from glacial meltwater can alter the ecological dynamics of lake ecosystems by influencing factors such

as nutrient enrichment (nitrogen and phosphorus), turbidity, and thermal conditions[65–69]. In addition, as ice cover limits the growth cycle and light availability in alpine lakes, the shorter ice cover duration greatly prolongs the phenology and promotes algal biomass[10,70,71]. Our results also confirmed that the FUI index, represents increased transparency around ~2000 CE, resulting in a deepening of photic zones for algal growth[72,73]. There are contentions that glacial meltwater, colder in temperature, might mitigate this effect, such as restricted the benthic organism growth (e.g., benthic algae, macrophytes and invertebrates)[48,68,74], but our observations suggest otherwise, with increasing lake surface temperature, the RoC in primary productivity and algal diversity pointing to a warming influence[55,68].

Over recent decades, the TP has seen a notable expansion in the number and total area of glacial lakes, with a 17.12% rise in their count and a 17.15% increase in their total area[75]. This expansion has been accompanied by decreased salinity and increased nutrient levels due to erosion and runoff, which collectively promote algal growth[76]. The widespread decline in water

salinity (mean salinity from 92.76 g L^{-1} to 42.00 g L^{-1} during 1970–2010 CE across the TP) has created favorable conditions for more organism and could greatly influence microbial richness, diversity, and evenness[76,77]. Our geochemical records from Guozha Co further illustrate this trend, with an accelerated nutrient enrichment and a decrease in salinity contributing to the burgeoning algal populations. A global rise in atmospheric nitrogen and phosphorus deposition may also have added to the nutrient load of these lakes, and provided additional nutrients to phytoplankton[78,79]. Furthermore, the wide "greening" across the TP has increased terrestrial biomass, potentially increasing allochthonous organic carbon input to lakes and impacting algal community metabolism[80–82]. This terrestrial biomass represents another potential source for export of organic carbon to lakes, which could further impact the composition and metabolism of algal communities[10].

Our findings, reinforced by SEM results, emphasize the significant impact of rising temperatures, mediated through glacial meltwater, on algal communities inhabiting glacier-fed lakes (Fig. 5). This study underscores the urgent need to understand and mitigate the consequences of rapid ecological changes in high-elevation lake environments amidst ongoing global climate change.

Conclusion and implication

Our study provides a rate-based perspective on long-term primary production and biodiversity dynamics in Tibetan glacier lakes, an underexplored yet crucial aspect of ecological response to climate change. By quantifying the pace of aquatic ecological shifts in relation to climate warming, our multi-decadal empirical analyses show that algal biomass and diversity have accelerated more rapidly than temperature increases since the 1980s, indicating that glacier-fed lake ecosystems are undergoing transformations faster than the regional warming. This divergence between climate change and ecosystem rate of change is expected to either continue or exacerbate, posing unpredictable outcomes for biodiversity and fundamental ecosystem services. In light of our findings, we propose several key strategies for the sustainable management of alpine lake ecosystems on the TP:

(1) Establishing integrated baseline conditions of glacier-fed lake ecosystems is urgently needed, allowing current deviations in lake ecosystem characteristics under rapid warming to be quantified and assessed. Such baseline information can be obtained through comprehensive paleolimnology studies, incorporating sedimentary pigments, fossil remains (e.g., diatoms, cladocera, chironomids), and environmental DNA to elucidate past and present species distribution, abundance, community composition, and biomass changes at multi-decade scales.

(2) Launching long-term monitoring programs that combine remote sensing and in-situ measurements of physical drivers and biological responses in glacier-fed lakes is essential. Such initiatives are critical to ensure ongoing data capture, facilitating informed assessments of alpine aquatic biodiversity and trends. Currently, long-term ecological monitoring of TP alpine lakes is insufficient and requires significant enhancement.

(3) Incorporating critical rates of change into assessments and management strategies is necessary to address challenges triggered by rapidly evolving alpine aquatic ecosystem in the Anthropocene. Management practices must shift from maintaining static conditions to the adaptive management of dynamic rates of ecological change. Both scientific inquiry and policy must strive to mitigate the gap between climate and ecological change rates, aspiring towards a sustainable development paradigm that operates within safe ecological thresholds.

The escalating pace of ecological change in glacial lake environments presents new challenges but also offers unprecedented opportunities to refine conservation and management approaches. By focusing on the RoC and understanding their implications, we can develop more resilient strategies to safeguard these critical ecosystems amidst the pressing threats of climate change.

Materials and methods
Study site and sampling
Guozha Co, located on the northwest TP at 5080 m a.s.l (Fig. 1a), exemplifies a typical glacier-fed lake (area: 248.44 km^2; maximum depth: 150 m; volume: 14.30 km^3; drainage area: 2369.40 km^2)[83]. The lake is primarily fed by meltwater from the Chongce ice cap and Guliya ice cap in the West Kunlun Mountain Glacier to the north (Fig. 1b). The lake's salinity measured at 2.46 g L^{-1} in August 2021 (classified as a saltwater lake, 1–35 g L^{-1}). A 2015 in-situ water quality survey characterized Guozha Co as mesotrophic[46]. The region, characterized by a semi-arid, alpine climate with an annual mean temperature of −7 °C, precipitation below 100 mm, and evaporation under 25 mm, has witnessed the widespread distribution of gravelly and sandy sediments formed by the deposition of glacial meltwater in the catchment, as well as the presence of sparse surface vegetation[84]. The rapid warming, which has significantly increased the regional mean temperature from −7.52 °C to −6.45 °C after ~2000 CE (t-test; $p < 0.001$) within the period of 1901–2021 CE (Supplementary Fig. 20), was reported to trigger major hydrological environment changes, including earlier lake-ice melting, glacier retreat, and lake expansion (Fig. 1c, d)[2,3].

In August 2021, a 39-cm length sediment core (GZC-21) was retrieved from the western part of Guozha Co at a water-depth of 76 m using UWITEC gravity corer. The sediment core was transported under refrigerated conditions and subsampled at 1-cm intervals in the laboratory. The middle sections, which were kept as fresh frozen samples, was used for sedaDNA analysis. Remaining samples were freeze-dried for photosynthetic pigment and geochemical analyses. All samples were stored at −20 °C in darkness to preserve their integrity before lab analyses.

Chronology and physicochemical analysis
The chronology of GZC-21 core was established using radioactive isotope ^{210}Pb and ^{137}Cs activities, measured at 1-cm intervals throughout the top 11 cm via gamma spectrometry (Hyperpure Ge detector). The age-depth model was constructed using the "serac" package in R-4.3.1 platform[85]. Sediment dry samples for total organic carbon (TOC, %) analysis were ground and pre-treated with 1 mol L^{-1} HCl to remove carbonates. TOC was measured using a Euro 3000 elemental analyzer, following the standard method described in Lin et al. (2020)[86]. Major and trace elements, including total phosphorous (mg kg^{-1}), were determined by sequential digestion of ground samples using inductively coupled plasma atomic emission spectrometry (ICP-AES; Leeman Labs, Profile DV) and inductively coupled plasma mass spectrometry (ICP-MS; Agilent 7700x)[86]. Low-frequency mass magnetic susceptibility (MS) (χ_{lf}, 10^{-8} m^3 kg^{-1}) was measured using a Bartington MS2 susceptibility meter at an operating frequency of 0.47 kHz (Supplementary Note 2).

Photosynthetic pigment analysis
Photosynthetic pigments comprising chlorophylls and carotenoids were quantified using an Agilent 1260 series high-performance liquid chromatography (HPLC) system following standard protocols[87,88]. Briefly, pigment extraction from sediment dry samples was conducted under freezing conditions via a 12-hour incubation with a mixed solvent of acetone, methanol, and deionized water. The extracts were filtered through a 0.2-μm PTEE syringe filter, completely dried under nitrogen, and redissolved in a mixture of acetone, ion pairing reagent (IPR, a mixture of tetrabutyl ammonium acetate and ammonium acetate in deionized water), and methanol. Sample injection into the HPLC system enabled separation of chlorophylls and carotenoids on a XDB-C18 column (4.6 × 150 mm, 5 μm particle size) using an Eclipse 120 quaternary pump, with detection performed via a photodiode array detector coupled to a fluorescence detector. Pigment concentrations were calculated by comparing peak areas against standards of known concentration and were expressed in nmole pigment g^{-1} TOC to calibrate organic degradation[73,89,90].

DNA extraction, amplification and sequencing

Strict laboratory protocols were followed to minimize cross-contamination during sample processing, DNA extraction, and polymerase chain reaction (PCR) amplification (Supplementary Note 7). Frozen samples from 27 distinct layers were subsampled at 1 cm intervals (~5 g) for *sed*aDNA analysis. PCR assays targeted two groups: the V4-V5 hypervariable region of the 16S rRNA gene (~370 bp) for cyanobacteria, amplified using primers 515F-926R[91]; and the V7 hypervariable region of the 18S rRNA gene (~260 bp) for micro-eukaryotes[42,92], amplified using primers 960F[93] and NSR1438[94]. Triplicate PCR reactions were performed for each DNA extract to ensure reproducibility, with negative controls included in all runs to monitor contamination. PCR products were visualized using 2% agarose gel electrophoresis. Sequencing was performed using NovaSeq (Illumina) PE250 by Shanghai Biozeron Biotechnology Co., Ltd. (Shanghai) (see Supplementary Note 7 for laboratory procedures).

Bioinformatics and biodiversity analysis

The quality-filtering of raw sequencing reads was performed using Trim-momatic (v.0.30); sequence merging was conducted with FLASH (v.1.2.7). Operational taxonomic unit (OTU) clustering was performed using Usearch (v.11.0.667) at a similarity threshold of 97% (Supplementary Note 7). Taxonomic annotation was conducted in QIIME 2 (v.2024.2) using the SILVA_138 database (confidence threshold = 80%). After depth normalization to the minimum sequencing depth, only OTUs corresponding to eukaryotic algae and cyanobacteria were retained, while non-algal OTUs were excluded. Alpha diversity metrics, including algal OTU richness and Shannon index, were calculated to evaluate within-sample diversity and temporal differences in algal communities. We employed beta diversity metrics, including non-metric multidimensional scaling (NMDS) using the metaMDS function and principal coordinate analysis (PCoA) using the ordinate function, specifying "bray" as the distance metric, to indicate community turnover. Log transformation was applied for algal *sed*aDNA data standardization. To statistically evaluate differences in community composition during different time periods, we conducted the PERMA-NOVA test using the adonis2 function. All diversity analyses were performed using the "*vegan*" package in R software (v.4.3.1)[95].

Multisource regional data compilation

Climate data (temperature) spanning 1901 to 2021 CE from the watershed were sourced and extracted from the Climate Research Unit (CRU) of the University of East Anglia (http://www.cru.uea.ac.uk/). Climate data for the past millennium were reconstructed from proxy-based records, including regional temperature ($\delta^{18}O$) and precipitation (glacier net accumulation) derived from Guliya ice core[96–99]. Additional environmental data, such as lake area/volume, glacier mass balance, and lake surface temperature, were obtained based on remote sensing and in-situ monitoring from the National Tibetan Plateau Data Center/Third Pole Environment Data Center (https://data.tpdc.ac.cn/) and the Big Earth Data Platform for Three Poles (https://data.casearth.cn/) (Supplementary Table 4). Furthermore, a dataset of remotely sensed Forel-Ule Index (FUI), as an integrated metric to represent the state of lake ecosystems[100], was downloaded, which focusing on lake area larger than 25 km^2 for TP inland waters during the period from 2000 to 2018 CE (Fig. 1a)[101]. We also collected the published paleoecological records covering the past two centuries (since ~1800 CE) from glacial lakes on the TP for regional comparison and integration (Supplementary Table 5). During the data collection process, we utilized major scientific databases, including Web of Science (https://webofscience.clarivate.cn/) and Elsevier ScienceDirect (https://www.sciencedirect.com/) (see Supplementary Note 8 for more information).

Numerical and model analyses of Community structure change and paleoenvironmental shift

We conducted the NMDS analysis based on Bray-Curtis distance to visualize dissimilarities and changes in structure in alga pigment assemblages (chlorophylls and carotenoids) and the *sed*aDNA dataset (eukaryotic

algae and cyanobacterial communities) using the "vegan" package in the R platform[95]. The principal component analysis (PCA) was performed on sediment element variables to extract components that capture the major variations in elemental composition. The Sequential t-test Analysis of Regime-Shifts (STRAS) with two tailed t-test ($p < 0.05$, cut-off length of 10 sequential time points) was applied to major paleoenvironmental time series to identify potential regime shifts in processes[102,103]. The identified sedimentary paleovariables mainly include TOC, TN, C/N, grain size, magnetic susceptibility and sediment elements.

Generalized additive model analysis

Generalized additive models (GAM) can flexibly simulate temporal dynamic change in data series by incorporating smooth functions of time[104]. GAM have been widely applied in modeling environmental and paleoe-cological time series[105,106]. We applied GAM with REML (restricted maximum likelihood), using the "*mgcv*" in R software[107], to analysis paleoecological variables including sediment pigments and *sed*aDNA time series from Guozha Co. Similarly, temporal trends in regional temperature changes were also estimated by the GAM.

For regional time series including lake FUI and the collected paleoe-cological records on the TP, hierarchical generalized additive models (HGAM) were employed to simulate their common temporal trends, since HGAM are more effective for analyzing grouped time series[108]. The selection of parameters setting for the GAM and HGAM analysis is followed the standard technical recommendations[104,108,109]. The residual autocorrelation and statistical summary are collectively used to evaluate the robustness of the modeling (Supplementary Note 9, Supplementary Figs. 21–24, Supplementary Table 6). All analyses were conducted using the "*mgcv*" package in R software[107].

Rate of change analysis

Sedimentary pigments and ancient DNA can accurately record the variability of algal communities through time[109], and thus reliably reflect changes in lake ecosystem variability under climate change. Temporal RoC in paleoecological time series (pigments and *sed*aDNA proxies) from Guozha Co and regional climate (temperature) was quantified from the posterior simulations of the fitted GAM using the first derivative of a spline[104]. Specifically, we first used the "*mgcv*" package in R to fit smooth GAM for the time-series data and applied function *predict()* to obtain the fitted values. We then calculated the first derivative of these fitted values via finite differences to represent the RoC, using functions *fderiv()* and *confint()* from the "*gratia*" package[110], we calculated the first derivative of these fitted values via finite differences to represent RoC. Periods of significant changes in variability were identified when the 95% CI of the derivative did not contain zero (Supplementary Note 9). To ensure comparability of the RoC, all time-series data, including ecological proxies (pigment, *sed*aDNA) and temperature, were standardized (Min-Max normalization) prior to GAM fitting. All GAM models fitting the selected time series contained a continuous-time first-order autoregressive [CAR(1)] process to account for temporal autocorrelation[104]. To further compare the trends between ecological rates and climate rates, we integrate the rate of all ecological indicators after RoC calculation, and carry out a 1:1 scale modeling with the temperature rate. Similarly, temporal rate of change in regional lake FUI and paleoecological time series was estimated from the posterior simulations of the fitted HGAM using the first derivative of a spline[104,108]. All RoC analyses were performed using the "*mgcv*" package in R (v.4.3.1).

Driver-response relationship analysis

Structural equation modeling (SEM) is a multivariate, hypothesis-driven technique that is based on a structural model representing a hypothesis about the causal relations among several variables[111]. SEM was employed to test our hypothesis regarding the cascading effects of climate warming on ecosystems. Specifically, SEM quantified the statistical relationships between environmental variables (temperature, precipitation, solar radiation, and glacial meltwater) and lake primary production (pigment

concentration of total algae), with the method of maximum likelihood estimation (MLE). To ensure consistency and alignment, all variables were resampled to match their temporal resolutions before inclusion in the SEM. Collinearity analysis was performed to exclude redundant variables and pathways with p-values < 0.05 were considered statistically significant. Model performance was assessed using key fit indices, including Normed Fit Index (NFI, > 0.9), Comparative Fit Index (CFI, > 0.9) and Akaike Information Criterion (AIC, the smaller the better). The SEM path analysis was conducted using the SPSS AMOS platform (Supplementary Note 10, Supplementary Fig. 25).

Reporting summary
Further information on research design is available in the Nature Portfolio Reporting Summary linked to this article.

Data availability
The sediment pigment, *sed*aDNA, and geochemical data used in this study can be found at https://figshare.com/s/ed3b20effa2b3778696c. The climate data (temperature) during the period from 1901 to 2021 CE can also be obtained from the Climate Research Unit (CRU) of the University of East Anglia (http://www.cru.uea.ac.uk/). For paleoclimatic record data in previous study, including the reconstructed data of temperature and precipitation, please refer to Supplementary Table 4. The data on the attributes of the watershed and the lake can also be retrieved from Supplementary Table 4 (the National Tibetan Plateau Data Center/Third Pole Environment Data Center (https://data.tpdc.ac.cn/) and the Big Earth Data Platform for Three Poles (https://data.casearth.cn/)). The regional intergration (meta-analysis) data, including the ecological records of glacial lakes on the Tibetan Plateau and the FUI, can be found in Supplementary Table 5 and are archived at https://figshare.com/s/ed3b20effa2b3778696c.

Code availability
The GAM/HGAM used in this study is an open-source model provided on https://github.com/eric-pedersen/mixed-effect-gams[104,108]. The example code of GAM/HGAM analysis and bioinformatics analysis is archived and available in https://github.com/DCL-prog/GAM-analysis.

References
1. Shugar, D. H. et al. Rapid worldwide growth of glacial lakes since 1990. *Nat. Clim. Change* **10**, 939–945 (2020).
2. Xu, F. et al. Widespread societal and ecological impacts from projected Tibetan Plateau lake expansion. *Nat. Geosci.* **17**, 516–523 (2024).
3. Yao, T. et al. The imbalance of the Asian water tower. *Nat. Rev. Earth Environ.* **3**, 618–632 (2022).
4. Zhang, G., Yao, T., Xie, H., Wang, W. & Yang, W. An inventory of glacial lakes in the Third Pole region and their changes in response to global warming. *Glob. Planet. Change* **131**, 148–157 (2015).
5. Qiu, J. China: The third pole. *Nature* **454**, 393–396 (2008).
6. Duan, J., Li, L. & Fang, Y. Seasonal spatial heterogeneity of warming rates on the Tibetan Plateau over the past 30 years. *Sci. Rep.* **5**, 11725 (2015).
7. Zhang, G. et al. Response of Tibetan Plateau lakes to climate change: trends, patterns, and mechanisms. *Earth-Sci. Rev.* **208**, 103269 (2020).
8. Song, C., Huang, B., Richards, K., Ke, L. & Hien Phan, V. Accelerated lake expansion on the Tibetan Plateau in the 2000s: Induced by glacial melting or other processes?. *Water Resour. Res.* **50**, 3170–3186 (2014).
9. Zhang, G. et al. Underestimated mass loss from lake-terminating glaciers in the greater Himalaya. *Nat. Geosci.* **16**, 333–338 (2023).
10. Woolway, R. I., et al. Global lake responses to climate change. *Nat. Rev. Earth Environ.* **1**, 388–403 (2020).
11. Huang, L., Woolway, R. I., Timmermann, A., Lee, S.-S., Rodgers, K. B. & Yamaguchi, R. Emergence of lake conditions that exceed natural temperature variability. *Nat. Geosci.* https://doi.org/10.1038/s41561-024-01491-5 (2024).
12. Huang, L., et al. Emerging unprecedented lake ice loss in climate change projections. *Nat. Commun.* **13**, 5798 (2022).
13. Zheng, G. et al. Increasing risk of glacial lake outburst floods from future Third Pole deglaciation. *Nat. Clim. Change* **11**, 411–417 (2021).
14. Zhang, T., Wang, W. & An, B. Heterogeneous changes in global glacial lakes under coupled climate warming and glacier thinning. *Commun. Earth Environ.* **5**, 374 (2024).
15. Liu, K. et al. Ongoing drainage reorganization driven by rapid lake growths on the Tibetan Plateau. *Geophys. Res. Lett.* **48**, e2021GL095795. 2021.
16. Bosson, J. B. et al. Future emergence of new ecosystems caused by glacial retreat. *Nature* **620**, 562–569 (2023).
17. Kohler, T. J. et al. Global emergent responses of stream microbial metabolism to glacier shrinkage. *Nat. Geosci.* https://doi.org/10.1038/s41561-024-01393-6 (2024).
18. Zhu, L. et al. Physical and biogeochemical responses of Tibetan Plateau lakes to climate change. *Nat. Rev. Earth Environ.* https://doi.org/10.1038/s43017-025-00650-5 (2025).
19. Ryo, M., Aguilar-Trigueros, C. A., Pinek, L., Muller, L. A. H. & Rillig, M. C. Basic principles of temporal dynamics. *Trends Ecol. Evol.* **34**, 723–733 (2019).
20. Steinbauer, M. J. et al. Accelerated increase in plant species richness on mountain summits is linked to warming. *Nature* **556**, 231–234 (2018).
21. Neate-Clegg, M. H. C., Tonelli, B. A. & Tingley, M. W. Advances in breeding phenology outpace latitudinal and elevational shifts for North American birds tracking temperature. *Nat. Ecol. Evol.* https://doi.org/10.1038/s41559-024-02536-z (2024).
22. Felton, A. J., et al. Climate disequilibrium dominates uncertainty in long-term projections of primary productivity. *Ecol. Lett.* **25**, 2688–2698 (2022).
23. Loehle, C. Disequilibrium and relaxation times for species responses to climate change. *Ecol. Model.* **384**, 23–29 (2018).
24. Chan, W.-P. et al. Climate velocities and species tracking in global mountain regions. *Nature.* https://doi.org/10.1038/s41586-024-07264-9 (2024).
25. Strack, A., Jonkers, L., C. Rillo, M., Hillebrand, H. & Kucera, M. Plankton response to global warming is characterized by non-uniform shifts in assemblage composition since the last ice age. *Nat. Ecol. Evol.* https://doi.org/10.1038/s41559-022-01888-8 (2022).
26. Williams, J. W., Ordonez, A. & Svenning, J.-C. A unifying framework for studying and managing climate-driven rates of ecological change. *Nat. Ecol. Evol.* **5**, 17–26 (2021).
27. Kuussaari, M. et al. Extinction debt: a challenge for biodiversity conservation. *Trends Ecol. Evol.* **24**, 564–571 (2009).
28. Cerini, F., Childs, D. Z. & Clements, C. F. A predictive timeline of wildlife population collapse. *Nat. Ecol. Evol.* **7**, 320–331 (2023).
29. Kraemer, B. M. et al. Climate change drives widespread shifts in lake thermal habitat. *Nat. Clim. Change* **11**, 521–529 (2021).
30. Zhang, Z. et al. Supraglacial and subglacial ecosystems contribute differently towards proglacial ecosystem communities in Kuoqionggangri Glacier, Tibetan Plateau. *Commun. Earth Environ.* **5**, 636 (2024).
31. Trisos, C. H., Merow, C. & Pigot, A. L. The projected timing of abrupt ecological disruption from climate change. *Nature* **580**, 496–501 (2020).

Article

32. Liu, K. et al. Glacier retreat induces contrasting shifts in bacterial biodiversity patterns in glacial lake water and sediment. *Microb. Ecol.* **87**, 128 (2024).

33. Liu, K. et al. Temperature-driven shifts in bacterioplankton biodiversity: Implications for cold-preferred species in warming Tibetan proglacial lakes. *Water Res.* **265**, 122263 (2024).

34. Ouyang, J. et al. Global warming induces the succession of photosynthetic microbial communities in a glacial lake on the Tibetan Plateau. *Water Res.* **242**, 120213 (2023).

35. Hastings, A. et al. Transient phenomena in ecology. *Science* **361**, eaat6412 (2018).

36. Mottl, O. et al. Rate-of-change analysis in paleoecology revisited: a new approach. *Rev. Palaeobot. Palynol.* **293**, 104483 (2021).

37. O'Reilly, C. M. et al. Rapid and highly variable warming of lake surface waters around the globe. *Geophys. Res. Lett.* **42** https://doi.org/10.1002/2015gl066235 (2015).

38. Pinek, L., Mansour, I., Lakovic, M., Ryo, M. & Rillig, M. C. Rate of environmental change across scales in ecology. *Biol. Rev.* **95**, 1798–1811 (2020).

39. Smol, J. P. Tracking long-term environmental changes in Arctic lakes and ponds: a paleolimnological perspective. *Arctic*. **58**, https://doi.org/10.14430/arctic421 (2010).

40. Capo, E. et al. Lake sedimentary DNA research on past terrestrial and aquatic biodiversity: overview and recommendations. *Quaternary* **4** (2021).

41. Stivrins, N. et al. Towards understanding the abundance of non-pollen palynomorphs: a comparison of fossil algae, algal pigments and *seda*DNA from temperate lake sediments. *Rev. Palaeobot. Palynol.* **249**, 9–15 (2018).

42. Capo, E. et al. Long-term dynamics in microbial eukaryotes communities: a palaeolimnological view based on sedimentary DNA. *Mol. Ecol.* **25**, 5925–5943 (2016).

43. Lan, J. et al. Time marker of 137Cs fallout maximum in lake sediments of Northwest China. *Quat. Sci. Rev.* **241**, 106413 (2020).

44. Ritchie, J. C. & Mchenry, J. R. Application of radioactive fallout Cesium-137 for measuring soil erosion and sediment accumulation rates and patterns: a review. *J. Environ. Qual.* **19**, 215–233 (1990).

45. Li, C.-G., et al. Quantitative estimates of Holocene glacier meltwater variations on the Western Tibetan Plateau. *Earth Planet. Sci. Lett.* **559**, 116766 (2021).

46. Liu, C. et al. In-situ water quality investigation of the lakes on the Tibetan Plateau. *Sci. Bull. (Beijing)* **66**, 1727–1730 (2021).

47. Huo, S., Zhang, H., Wang, J., Chen, J. & Wu, F. Temperature and precipitation dominates millennium changes of eukaryotic algal communities in Lake Yamzhog Yumco, Southern Tibetan Plateau. *Sci. Total Environ.* **829**, 154636 (2022).

48. He, J. et al. Responses of lake diatoms to rapid 21st century warming on the southeastern Tibetan Plateau. *Anthropocene* **39**, 100345 (2022).

49. Wang, Q., Wang, R., Yang, X., Anderson, N. J. & Kong, L. Interactive effects of climate-atmospheric cycling on aquatic communities and ecosystem shifts in mountain lakes of southeastern Tibetan Plateau. *Sci. Total Environ.* **914**, 169825 (2024).

50. Han, W. et al. Anthropogenic activities altering the ecosystem in Lake Yamzhog Yumco, southern Qinghai-Tibetan Plateau. *Sci. Total Environ.* **904**, 166715 (2023).

51. Jia, J. et al. Evolving geographical gross primary productivity patterns in global lake systems and controlling mechanisms of associated phytoplankton communities since the 1950s. *Earth-Sci. Rev.* **234**, 104221 (2022).

52. Brown, J. H., Gillooly, J. F., Allen, A. P., Savage, V. M. & West, G. B. Toward a metabolic theory of ecology. *Ecology* **85**, 1771–1789 (2004).

53. Liu, K. et al. Temporal variability of microbial communities during the past 600 years in a Tibetan lake sediment core. *Palaeogeogr. Palaeoclimatol. Palaeoecol.* **584**, 110678 (2021).

54. Liang, J. et al. Lake ecosystem on the Qinghai–Tibetan Plateau severely altered by climatic warming and human activity. *Palaeogeogr. Palaeoclimatol. Palaeoecol.* **576**, 110509 (2021).

55. Lin, X., Rioual, P., Peng, W., Yang, H. & Huang, X. Impact of recent climate change on Lake Kanas, Altai Mountains (N.W. China) inferred from diatom and geochemical evidence. *J. Paleolimnol.* **59**, 461–477 (2018).

56. Jia, W. et al. Sedimentary ancient DNA reveals past ecosystem and biodiversity changes on the Tibetan Plateau: Overview and prospects. *Quat. Sci. Rev.* **293**, 107703 (2022).

57. Wilson, G. P., et al. Diatom response to the Last Glacial–Interglacial Transition in the Ioannina basin, northwest Greece: implications for Mediterranean palaeoclimate reconstruction. *Quat. Sci. Rev.* **27**, 428–440 (2008).

58. RÜHland, K., Paterson, A. M. & Smol, J. P. Hemispheric-scale patterns of climate-related shifts in planktonic diatoms from North American and European lakes. *Glob. Change Biol.* **14**, 2740–2754 (2008).

59. Hébert, M.-P., Beisner, B. E., Rautio, M. & Fussmann, G. F. Warming winters in lakes: Later ice onset promotes consumer overwintering and shapes springtime planktonic food webs. *Proc. Natl. Acad. Sci.* **118**, e2114840118 (2021).

60. Lin, Q., et al. Responses of trophic structure and zooplankton community to salinity and temperature in Tibetan lakes: Implication for the effect of climate warming. *Water Res* **124**, 618–629 (2017).

61. Gil, M. A., Baskett, M. L., Munch, S. B. & Hein, A. M. Fast behavioral feedbacks make ecosystems sensitive to pace and not just magnitude of anthropogenic environmental change. *Proc. Natl Acad. Sci.* **117**, 25580–25589 (2020).

62. Beck, K. K. et al. Variance and rate-of-change as early warning signals for a critical transition in an aquatic ecosystem state: a test case from Tasmania, Australia. *J. Geophys. Res.: Biogeosci.* **123**, 495–508 (2018).

63. Sun, F., He, B., Liu, C. & Zeng, Y. Comparison of hydrological patterns between glacier-fed and non-glacier-fed lakes on the southeastern Tibetan Plateau. *Remote Sensing*. **13**, https://doi.org/10.3390/rs13204024 (2021).

64. Bhattacharya, A. et al. High Mountain Asian glacier response to climate revealed by multi-temporal satellite observations since the 1960s. *Nat. Commun.* **12**, 4133 (2021).

65. Slemmons, K. E. H. The Influence of Glacial Meltwater on Alpine and Arctic Lake Phytoplankton Throughout the Holocene. Electronic Theses and Dissertations. https://digitalcommons.library.umaine.edu/etd/2005 (2013).

66. Stibal, M. et al. Glacial ecosystems are essential to understanding biodiversity responses to glacier retreat. *Nat. Ecol. Evol.* **4**, 686–687 (2020).

67. Shi, S. et al. Sedimentary organic molecular compositions reveal the influence of glacier retreat on ecology on the Tibetan Plateau. *Sci. Total Environ.* **882**, 163629 (2023).

68. Li, Y., et al. Influence of Lateglacial meltwater influx from alpine glaciers on the aquatic ecosystem of Kanas Lake in the Altai Mountains, China. *Palaeogeogr. Palaeoclimatol. Palaeoecol.* **604**, 111214 (2022).

69. Slemmons, K. E. H. & Saros, J. E. Implications of nitrogen-rich glacial meltwater for phytoplankton diversity and productivity in alpine lakes. *Limnol. Oceanogr.* **57**, 1651–1663 (2012).

70. Wu, Y. et al. Ice phenology dataset reconstructed from remote sensing and modelling for lakes over the Tibetan Plateau. *Sci. Data* **9**, 743 (2022).

71. Caramatti, I., Peeters, F., Hamilton, D. & Hofmann, H. Modelling inter-annual and spatial variability of ice cover in a temperate lake with complex morphology. *Hydrol. Process.* **34**, 691–704 (2020).

72. Röthig, T. et al. Human-induced salinity changes impact marine organisms and ecosystems. *Glob. Change Biol.* **29**, 4731–4749 (2023).

73. Lin, Q., Zhang, K., McGowan, S., Capo, E. & Shen, J. Synergistic impacts of nutrient enrichment and climate change on long-term water quality and ecological dynamics in contrasting shallow-lake zones. *Limnol. Oceanogr.* **66**, 3271–3286 (2021).

74. Slemmons, K. E. H., Saros, J. E. & Simon, K. The influence of glacial meltwater on alpine aquatic ecosystems: a review. *Environ. Sci. Process. impacts* **15**, 1794–1806 (2013).

75. Dou, X. et al. Spatio-temporal evolution of glacial lakes in the Tibetan Plateau over the past 30 years. *Remote Sens.* **15**, 416 (2023).

76. Song, C., et al. Widespread declines in water salinity of the endorheic Tibetan Plateau lakes. *Environ. Res. Commun.* **4**, 091002 (2022).

77. Liu, C., et al. The decrease of salinity in lakes on the Tibetan Plateau between 2000 and 2019 based on remote sensing model inversions. *Int. J. Digital Earth* **16**, 2644–2659 (2023).

78. Hu, Z. J., Anderson, N. J., Yang, X. D. & McGowan, S. Catchment-mediated atmospheric nitrogen deposition drives ecological change in two alpine lakes in SE Tibet. *Global Change Biol.* **20**, 1614–1628 (2014).

79. Zhang, X., Lin, C. & Liu, E. C. X. Atmospheric dry deposition of nitrogen and phosphorus in Lake Qinghai, Tibet Plateau. *Atmos. Pollut. Res.* **13**, 101481 (2022).

80. Zhang, W., Zhou, T. & Zhang, L. Wetting and greening Tibetan Plateau in early summer in recent decades. *J. Geophys. Res.: Atmos.* **122**, 5808–5822 (2017).

81. Li, J., et al. Weakening warming on spring freeze–thaw cycle caused greening Earth's third pole. *Proc. Natl Acad. Sci.* **121**, e2319581121 (2024).

82. Huang, R. et al. Significant greening in the western Tibetan Plateau and surroundings occurred after the 1970s. *Commun. Earth Environ.* **6**, 82 (2025).

83. Qiao, B., et al. Estimation of lakes water storage and their changes on the northwestern Tibetan Plateau based on bathymetric and Landsat data and driving force analyses. *Quat. Int.* **454**, 56–67 (2017).

84. Li, C.-G., et al. Refined dating using palaeomagnetic secular variations on a lake sediment core from Guozha Co, northwestern Tibetan Plateau. *Quat. Geochronol.* **62**, 101146 (2021).

85. Bruel, R. & Sabatier, P. serac: an R package for ShortlivEd RAdionuclide chronology of recent sediment cores. *J. Environ. Radioactivity* **225**, 106449 (2020).

86. Lin, Q., et al. Deciphering centurial anthropogenic pollution processes in large lakes dominated by socio-economic impacts. *Anthropocene* **32**, 100269 (2020).

87. McGowan, S. in *Encyclopedia of Quaternary Science* 2nd edn., 326–338 (Elsevier, 2013).

88. Leavitt, P. R. & Hodgson, D. A. in *Tracking Environmental Change Using Lake Sediments: Terrestrial, Algal, and Siliceous Indicators* (eds Smol, J. P., Birks, J. B. & Last, W. M.) 295–325 (2001).

89. Huang, S., Zhang, K., Lin, Q., Kattel, G. & Shen, J. Lake ecosystem regime shifts induced by agricultural intensification: a century scale paleolimnological investigation from the Huai River Basin (China). *Quat. Sci. Rev.* **285**, 107522 (2022).

90. Du, C., et al. Glacier meltwater input and salinity decline promote algal growth in a Tibetan Saline Lake. *Freshw. Biol.* **70**, e70010 (2025).

91. Parada, A. E., Needham, D. M. & Fuhrman, J. A. Every base matters: assessing small subunit rRNA primers for marine microbiomes with mock communities, time series and global field samples. *Environ. Microbiol.* **18**, 1403–1414 (2016).

92. Capo, E., et al. Tracking a century of changes in microbial eukaryotic diversity in lakes driven by nutrient enrichment and climate warming. *Environ. Microbiol.* **19**, 2873–2892 (2017).

93. Gast, R. ebeccaJ., Dennett, M. arkR. & Caron, D. avidA. Characterization of protistan assemblages in the Ross Sea, Antarctica, by denaturing gradient gel electrophoresis. *Appl. Environ. Microbiol.* **70**, 2028–2037 (2004).

94. Van de Peer, Y., De Rijk, P., Wuyts, J., Winkelmans, T. & De Wachter, R. The European small subunit ribosomal RNA database. *Nucleic Acids Res.* **28**, 175–176 (2000).

95. Oksanen, J. et al. *Vegan Community Ecology* package version 2.6-2 April 2022 (2022).

96. Thompson, L. G. et al. Ice core records of climate variability on the Third Pole with emphasis on the Guliya ice cap, western Kunlun Mountains. *Quat. Sci. Rev.* **188**, 1–14 (2018).

97. Thompson, L. G. et al. Abrupt tropical climate change: Past and present. *Proc. Natl Acad. Sci.* **103**, 10536–10543 (2006).

98. Thompson, L. G. et al. Tropical climate instability: the last glacial cycle from a Qinghai-Tibetan ice core. *Science* **276**, 1821–1825 (1997).

99. Bao Y., Braeuning A., Yafeng S., Fahu C. Evidence for a late Holocene warm and humid climate period and environmental characteristics in the arid zones of northwest China during 2.2 ∼ 1.8 kyr B.P. *J. Geophys. Res.: Atmos*. **109**, https://doi.org/10.1029/2003JD003787 (2004).

100. Han, Y., et al. Human Impacts Dominate Global Loss of Lake Ecosystem Resilience. *Geophys. Res. Lett.* **51**, e2024GL109298. 2024.

101. Wang, S. et al. A dataset of remote-sensed Forel-Ule Index for global inland waters during 2000–2018. *Sci. Data* **8**, 26 (2021).

102. Rodionov S. N. Use of prewhitening in climate regime shift detection. *Geophys. Res. Lett.* **33**, https://doi.org/10.1029/2006GL025904 (2006).

103. Howard, J. A. E., Jarre, A., Clark, A. E. & Moloney, C. L. Application of the sequential t-test algorithm for analysing regime shifts to the southern Benguela ecosystem. *Afr. J. Mar. Sci.* **29**, 437–451 (2007).

104. Simpson G. L. Modelling palaeoecological time series using Generalised Additive Models. *Front. Ecol. Evol.* **6**, https://doi.org/10.3389/fevo.2018.00149 (2018).

105. Benito X. et al. Ecological resilience in tropical Andean lakes: a paleolimnological perspective. *Limnol. Oceanogr.* **67**, https://doi.org/10.1002/lno.11747 (2021).

106. Swann, G. E. A. et al. Changing nutrient cycling in Lake Baikal, the world's oldest lake. *Proc. Natl Acad. Sci.* **117**, 27211–27217 (2020).

107. Wood, S. N. *Generalized Additive Models: An Introduction with R* 2nd edn. (Chapman and Hall/CRC). https://doi.org/10.1201/9781315370279 (2017).

108. Pedersen E. J., Miller D. L., Simpson G. L. & Ross. N. Hierarchical generalized additive models in ecology: an introduction with mgcv. https://doi.org/10.7717/peerj.6876/fig-1 (2019).

109. Lin, Q. et al. Transient social–ecological dynamics reveal signals of decoupling in a highly disturbed Anthropocene landscape. *Proc. Natl Acad. Sci.* **121**, e2321303121 (2024).

110. Simpson G. L. gratia: An R package for exploring generalized additive models. *J. Open Source Softw*. **9**, https://doi.org/10.21105/joss.06962 (2024)

111. Nettle, D. Ecological influences on human behavioural diversity: a review of recent findings. *Trends Ecol. Evol.* **24**, 618–624 (2009).

Acknowledgements

Author contributions

K.Z. and J.S. designed the study. C.D. performed the analysis, with additional support from K.Z., Q.L., S.H., Y.H., J.R., P.X., J.L., D.T., and J.S. on datasets and analytical approaches. All co-authors contributed to interpreting the data and writing the paper.

Competing interests

The authors declare no competing interests.

Additional information

Supplementary information The online version contains supplementary material available at https://doi.org/10.1038/s43247-025-02443-6.

Correspondence and requests for materials should be addressed to Ke Zhang or Ji Shen.

Peer review information *Communications Earth & Environment* thanks Lasse Topstad and the other, anonymous, reviewer(s) for their contribution to the peer review of this work. Primary Handling Editors: José Luis Iriarte Machuca, Somaparna Ghosh [A peer review file is available].

Reprints and permissions information is available at http://www.nature.com/reprints

Publisher's note Springer Nature remains neutral with regard to jurisdictional claims in published maps and institutional affiliations.